

N. BOUKOS<sup>1,✉</sup>  
C. CHANDRINO<sup>1</sup>  
K. GIANNAKOPOULOS<sup>1</sup>  
G. PISTOLIS<sup>2</sup>  
A. TRAVLOS<sup>1</sup>

# Growth of ZnO nanorods by a simple chemical method

<sup>1</sup> Institute of Materials Science, National Center for Scientific Research "Demokritos",  
15310 Ag. Paraskevi, Athens, Greece

<sup>2</sup> Institute of Physical Chemistry, National Center for Scientific Research "Demokritos",  
15310 Ag. Paraskevi, Athens, Greece

Received: 28 September 2005/Accepted: 13 January 2007  
© Springer-Verlag 2007

**ABSTRACT** ZnO nanorods were grown by a near-room-temperature, simple, chemical solution method on large-area Zn foils and substrate materials such as silicon, and zinc oxide thin films on silicon and glass. Study of the ZnO nanorods on the different substrates by electron microscopy methods shows that the morphology and size of the ZnO nanorods can be tuned varying the growth parameters and the substrates used. The growth mechanism is briefly discussed. Photoluminescence experiments at room temperature reveal a major emission peak of the nanorods at around 385 nm, which is attributed to the band edge transition of ZnO and weaker defect-related visible band peaks.

PACS 81.05.Dz; 78.55.Et; 81.07.-b

## 1 Introduction

In recent years, there has been growing research interest for semiconducting nanostructures because they can be used for fundamental studies of the role of size and dimensionality in their physical properties as well as their potential applications in optoelectronic nanodevices and functional materials [1]. ZnO is a direct wide band gap semiconductor (3.37 eV) with a wurtzite structure [2]. Due to its high exciton binding energy of 60 meV room-temperature ultraviolet lasing has been demonstrated [3]. ZnO epitaxial films and nanostructures have been widely studied for applications such as UV emitters, solar cells, gas sensors, varistors and surface electro-acoustic wave devices [1]. Various methods have been used for the production of ZnO nanostructures. They can be grouped in two main categories: high-temperature techniques, such as chemical vapor deposition, pulsed-laser deposition and thermal evaporation [4–7] where the growth temperature is higher than 400 °C, and chemical solution methods at around 100 °C [8–10]. The first category utilizes expensive equipment and is energy consuming, while the latter often require liquid-phase coating of the substrates with ZnO seeds, a procedure that is quite complex [11, 12].

In this paper we report the application of a near-room-temperature chemical solution method [9, 13] for the produc-

tion of ZnO nanorods in large-area substrates. The substrates used include silicon, zinc, and ZnO thin films on silicon and glass. This method is simple, does not use materials that can act as impurities (such as other anions from Zn salts) and can be varied in order to tune the dimensions of the ZnO nanorods.

## 2 Experimental

Fresh zinc foils with a purity of 99.9% were used as a reagent for the direct growth of ZnO nanorods on the substrates. The zinc foils were carefully cleaned with absolute alcohol and de-ionized water in an ultrasound bath. The substrates used were (111) Si, glass and Zn foil. We also prepared (111) Si and glass substrates where we had evaporated a 100 nm thin film of ZnO by electron beam. Typically a solution of analytical-grade formamide in distilled water was prepared and the Zn foil and substrate were immersed in the solution for a period 1 to 24 h. The concentration of formamide varied between 1–10 vol %. The solution was kept at a temperature in the range of 40–80 °C. The samples were taken out of the solution and rinsed in de-ionized water.

The samples were characterized with scanning electron microscopy (SEM) using a Philips 515 SEM and powder X-ray diffraction utilizing a Siemens D-500 diffractometer with Cu  $K_{\alpha}$  radiation ( $\lambda = 0.15418$  nm). Transmission electron microscopy (TEM) micrographs, electron diffraction patterns and high resolution TEM images were recorded with a Philips CM20 microscope operating at 200 kV. The photoluminescence measurements were carried out with a Perkin Elmer LS50 luminescence spectrometer at room temperature with 325-nm excitation.

## 3 Results and discussion

First the results concerning the growth of ZnO nanorods on Zn foil will be presented.

Figure 1 shows a top-view SEM image of the ZnO nanorods grown on the Zn foil after 20 h. It can be seen that the ZnO nanorods uniformly cover the Zn foil substrate. Their mean diameter is about 200 nm and their length is about 2  $\mu$ m. The rods grow approximately perpendicular to the substrate surface and their shape is hexagonal. The top tips of the nanorods show a flat hexagonal section. We have studied several ZnO nanorods by TEM in order to derive conclusions regarding their structure and crystallinity. This examination

✉ Fax: +30 210 6519430, E-mail: nboukos@ims.demokritos.gr

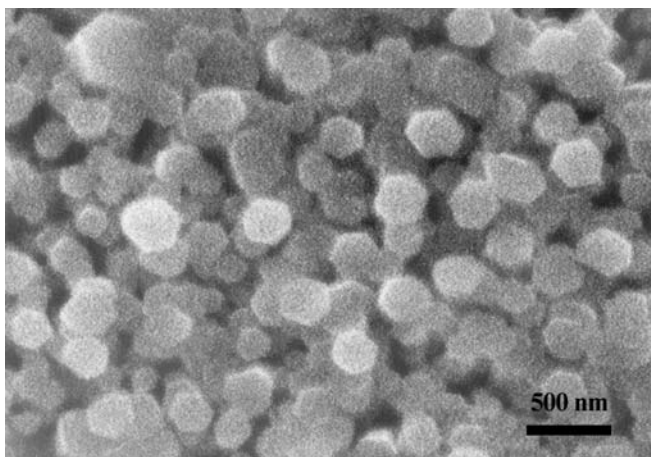


FIGURE 1 Top-view SEM image of ZnO nanorods

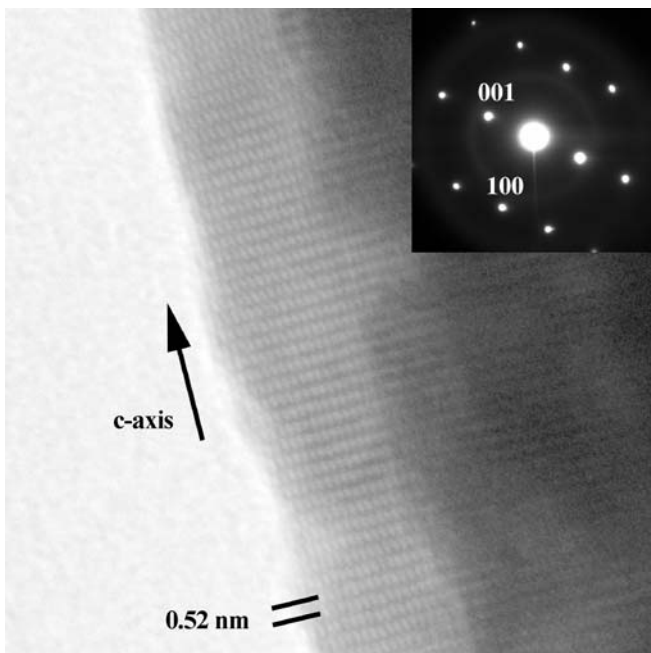


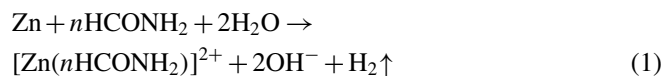
FIGURE 2 High-resolution TEM image of a ZnO nanorod grown on Zn foil and corresponding selected area electron diffraction pattern shown in the inset

showed that the ZnO nanorods have a hexagonal wurtzite structure with  $a = 0.325$  nm and  $c = 0.521$  nm. The inset of Fig. 2 shows a typical selected area electron diffraction pattern obtained from a ZnO nanorod. The electron beam is parallel to the  $[100]$  zone axis and the pattern indicates that the nanorod is single-crystalline. Their growth direction was examined by high-resolution TEM. In Fig. 2 a high-resolution TEM image near the side wall of a nanorod is presented. The interplanar spacing of 0.52 and 0.28 nm are clearly resolved and correspond to the lattice spacing of (001) and (010) ZnO planes, respectively. Consequently, we conclude that the nanorods grow along their  $c$ -axis.

Next we tried to grow ZnO on bare (111) Si substrates. In Fig. 3a the ZnO nanostructures grown at a temperature of 65 °C can be seen in 60° inclined view. There is a rather uniform coverage of the Si substrate surface with ZnO nanorods. They obtain hexagonal prismatic shapes and in some cases

“T-branches”. On rare occasions they have a “dendrite-like” shape, as the one shown in the middle of Fig. 3a. Their top tips are flat. They grow at various angles in respect to the Si substrate. Their length is 3–3.5  $\mu\text{m}$  and their diameter varies in the range 350–450 nm. As in the case of ZnO grown on Zn foil, we have studied their structure and crystallinity by TEM and we obtained the same results, i.e., the rods and each branch are single-crystalline and they grow along the  $c$  wurtzite axis. Comparing the ZnO nanostructures grown on Zn foil and bare Si substrates (Figs. 1 and 3a), it can be noticed that the ZnO nanorods in the first case are more dense, smaller in diameter, and approximately parallel to each other.

In order to understand the differences in the ZnO morphology, we have to outline the nucleation and growth mechanism. The otherwise remarkably slow zinc oxidation process, due to the formation of a passive ZnO thin layer, can be accelerated by the addition of formamide in the reaction solution. This forms Zn complexes (1), which subsequently release Zn ions for the consequential formation of zinc oxide. Further acceleration to the reaction process is achieved by performing the reaction at elevated temperatures.



Zinc-formamide complexes are continuously supplied from the zinc foil and can dissociate thermally to produce zinc ions that readily oxidize. The concentration of the zinc ions in the solution depends on the temperature and the formamide concentration [13]. ZnO can nucleate either homogeneously in the solution or heterogeneously on a proper surface. Usually homogeneous nucleation of solid phases (metal oxide in particular) has a higher activation energy barrier and consequently heterogeneous nucleation is more favorable. The reason for preferred nucleation on a substrate surface as compared with homogeneous nucleation in the solution is that the interfacial energy between crystal and substrate surface is usually smaller than between the crystal and solution. As a result, nucleation on the substrate occurs at a lower saturation than in the solution [14]. The nuclei on the substrate act as favorable sites for further ZnO growth. The ZnO wurtzite hexagonal structure is characterized of polar and non-polar surfaces and has no center of inversion and, consequently, the growth rate of various planes differs, i.e.,  $(001) < (10-1) < (100)$  [15, 16], leading to columnar growth along the  $c$ -axis. In the case of bare (111) Si substrate, the nucleation sites on its surface are scarcer compared to the polycrystalline Zn foil substrate and therefore fewer and bigger in diameter nanorods grow. The fact that the nanorods grow at various angles with respect to the Si substrate could be attributed to the high misfit of the basal plane of ZnO and (111) Si planes, resulting in non  $c$ -preferred oriented initial ZnO nuclei. It should be mentioned that even though perpendicular growth of ZnO rods on bare (100) Si substrate has been reported by Wu and Liu [17] they have employed chemical vapor deposition at 500 °C. Apart from the fact that nucleation in that case occurs from vapor, the use of high temperature resulted in an amorphous SiO<sub>2</sub> interfacial layer where no misfit occurs. The “T-branches” observed in some ZnO rods might be ascribed to twinning occurring in the relatively big rods that act as sec-

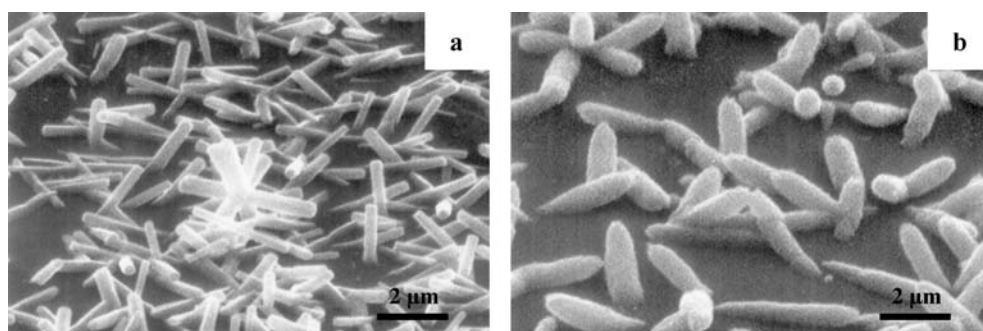


**FIGURE 3** Inclined-view SEM image of ZnO nanorods grown on bare (111) Si substrate at (a) 65 °C and (b) 80 °C

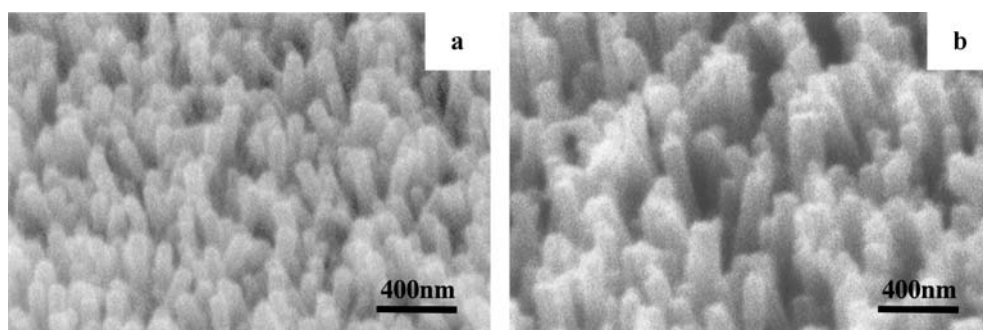


**FIGURE 4** Inclined-view SEM image of (a) thinner and (b) thicker ZnO nanorods grown on ZnO thin film/glass substrate using different growth conditions

ondary sites for the growth of rods perpendicular to the main one [18, 19].

Next, the influence of formamide solution temperature was studied. Figure 3b shows the ZnO rods grown at a temperature of 80 °C on bare (111) Si. They have a “cigar-like” shape, a length in the range 3–4 μm and diameter 650–800 nm and end up in an irregular-shaped tip and grow at various angles with respect to the Si surface. Comparing Fig. 3a and b, it is evident that as the solution temperature increases, the ZnO rods become bigger and their shape deviate from hexagonal, and this could be explained as follows. The higher temperature results in an increased concentration of Zn-formamide complexes in the solution which in turn enhances Zn supply for the formation of the ZnO rods. This supersaturation may perturb the way the growth units are incorporated in the crystal during ZnO rod growth, i.e., the relative growth rate of ZnO planes [16] and consequently give rise to the “cigar-like” morphology observed.

Finally, the influence of the growth nucleus density on the substrate was investigated. We choose to grow a ZnO thin film on glass and Si by electron beam evaporation at room temperature, as this method produces a very high density of nuclei and can also be applied in different technologically important substrates including ITO and plastics. In Fig. 4a, the ZnO nanorods grown on glass at a temperature of 65 °C can be seen. There is a high density of ZnO nanorods that grow almost perpendicular to the substrate. Their average diameter is about 80 nm and their length in the range of 1.5–2 μm. X-ray diffraction, Fig. 5a, verified that their structure is hexagonal wurtzite (JCPDS card no. 36-1451). In Fig. 5c, the relative peak intensities of the standard powder diffraction pattern of bulk ZnO are presented. The relative peak intensities of our spectrum are different, i.e., the (002) is the strongest one with a full width at half maximum of 0.17°, while the other peaks are very weak or not detected. This is an indi-

cation of a highly preferential growth perpendicular to the substrate and of very good *c*-axis alignment of the nanorods over a large substrate area. It should be mentioned that the effect of the underlying ZnO thin film is minimal, as can be seen in Fig. 5b where the X-ray diffraction spectrum of the ZnO thin film/glass substrate used for the subsequent growth of the ZnO nanorods, vertically displaced for clarity, is presented.

Figure 6a is a typical bright field TEM micrograph of a ZnO nanorod. It can be seen that the side walls of the nanorod are straight and parallel. The selected area electron diffraction pattern with zone axis [100], shown in the inset, verifies that is single-crystalline. In Fig. 6b, a high-resolution TEM image near the side wall of the nanorod is presented. The

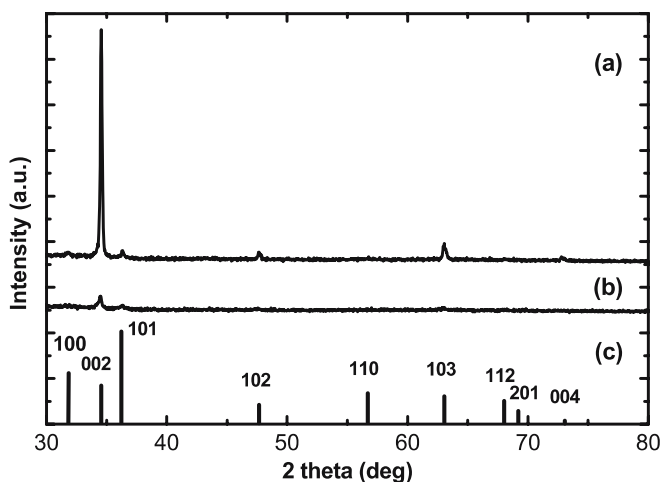


**FIGURE 5** X-ray diffraction spectrum of (a) ZnO nanorods grown on ZnO thin film/glass substrate, (b) ZnO thin film/glass substrate and (c) standard ZnO (JCPDS no. 36-1451)

(001) and (010) planes are imaged showing that the growth direction is along the  $c$ -axis as in the other cases examined in this study. It must be mentioned that the diameter of the nanorods can be tuned by varying the growth conditions. Figure 4b shows a SEM image of the nanorods grown with a different formamide concentration for the same growth time. Their mean diameter is about 120 nm and their length 1.5–2  $\mu\text{m}$ . The different formamide concentration may alter the relative growth speeds along the primary ZnO directions and consequently change the resulting aspect ratio of the nanorods.

Finally, it must be mentioned that analogous results were obtained for the growth of ZnO nanorods on (111) Si with a ZnO thin film.

Next we studied the room temperature photoluminescence of the ZnO nanorods. In Fig. 7 the photoluminescence spectra, obtained with 325 nm excitation (Xe lamp), of the samples are presented. Four individual peaks can be distinguished: A major peak at 385 nm and three minor ones at 422, 480, and 530 nm. The UV peak can be attributed to the exciton recombination related near band edge emission of ZnO [20].

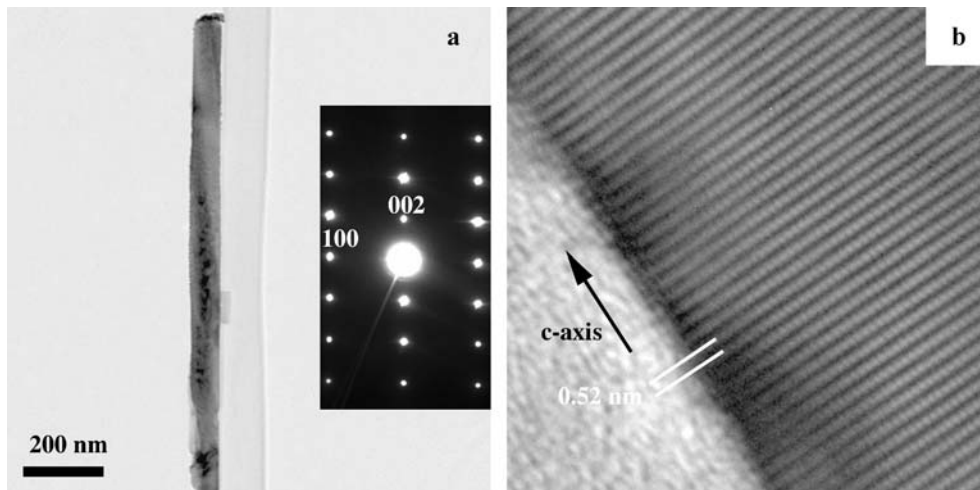


**FIGURE 6** (a) Bright-field TEM micrograph of a ZnO nanorod grown on ZnO thin film/glass substrate and corresponding selected area electron diffraction pattern shown in the *in-set*. (b) High-resolution TEM image of the same ZnO nanorod

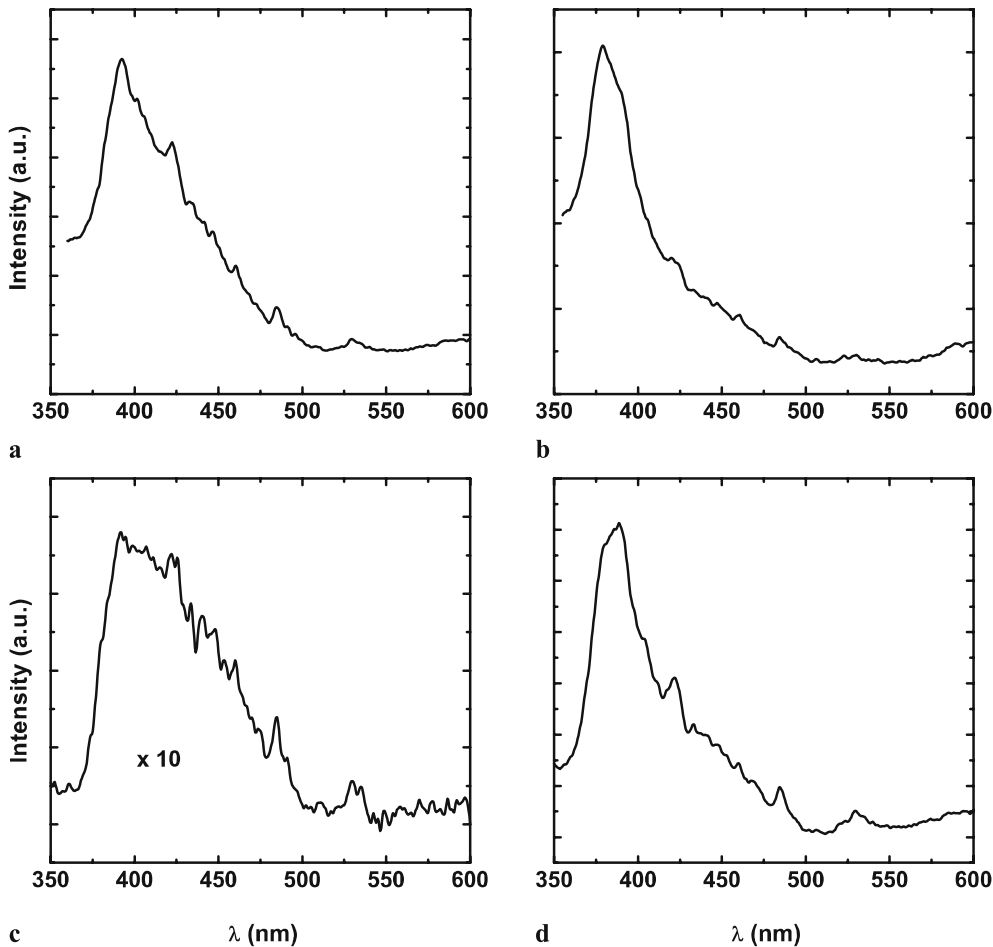


**FIGURE 7** Room-temperature photoluminescence spectra of ZnO nanorods grown on (a) Zn foil, bare (111) Si substrate at (b) 65 °C and (c) 80 °C and (d) ZnO thin film/glass substrate

The violet band emission at 420 nm has been reported by Jin et al. [21] in ZnO thin films. They assigned it to transitions between radiative defects, related to the interface traps existing at grain boundaries and the valence band. Since the ZnO nanorods in our study are single-crystalline, this explanation may be excluded. Xu et al. [22] have calculated the energy levels of various intrinsic defects in ZnO by the full potential linear muffin-tin orbital method. Their calculation showed an energy interval of 2.9 eV between the valence band and interstitial zinc. This value compares with the violet peak at 422 nm (2.93 eV) observed in our spectra. Consequently, the violet peak could be attributed to this transition. It must be mentioned that Fan et al. [23] have attributed the 424 nm peak in their photoluminescence spectra to the same transition. The blue 480 nm peak, to the best of our knowledge, has only been reported by Mahamuni et al. [24]. In accordance with them, we may possibly attribute it to the transition between oxygen vacancy and interstitial oxygen. Finally, the green band peak at 530 nm could be attributed to recombination of electrons in singly occupied oxygen vacancies with photoexcited holes [25].

A comparison between the spectra of Fig. 7 shows that ZnO rods grown on bare (111) Si at high temperature have more defect states, especially those that give rise to the 425 nm peak, while the nanorods grown on ZnO thin film/glass substrate have fewer. Apart from the ZnO rods grown on bare (111) Si at high temperature, all other samples show comparatively low level defect related emission indicating a relatively good overall quality of the ZnO nanorods.

#### 4 Conclusions

A simple, near-room-temperature chemical solution method is applied for the production of ZnO nanorods on large-area Zn foils and substrate materials such as silicon and zinc oxide thin films on silicon and glass. This method uses Zn foil as the zinc source and aqueous solution of formamide for the formation, transport, and thermal decomposition of zinc-formamide complexes to produce ZnO nanorods. Electron microscopy study shows that while the nanorods are single-crystalline, their morphology and size can be tuned vary-

ing the growth parameters and the substrates used. The ZnO nanorods grown on ZnO thin film/glass substrate have the higher aspect ratio and are characterized by a highly preferential growth perpendicular to the substrate and very good *c*-axis alignment. The anisotropic growth mechanism of the ZnO nanorods is discussed. Finally, the room-temperature photoluminescence being measured is characterized by a dominant near band edge peak and weaker defect-related visible band peaks.

#### REFERENCES

- 1 U. Oezguer, Y. Alivov, C. Liu, A. Teke, M. Reshchikov, S. Dogan, V. Avrutin, S. Cho, H. Morkoc, *J. Appl. Phys.* **98**, 041 301 (2005)
- 2 H. Chick, J. Liang, S. Cloutier, N. Kouklin, J. Xu, *Appl. Phys. Lett.* **84**, 3376 (2004)
- 3 M.H. Huang, S. Mao, H. Feick, H. Yan, Y. Wu, H. Kind, E. Weber, R. Russo, P. Yang, *Science* **292**, 1897 (2001)
- 4 W. Park, G. Yi, M. Kim, S. Pennycook, *Adv. Mater.* **14**, 1841 (2002)
- 5 Y. Kong, D. Yu, B. Zhang, W. Fang, S. Feng, *Appl. Phys. Lett.* **78**, 407 (2001)
- 6 H. Zhang, X. Sun, R. Wang, D. Yu, *J. Cryst. Growth* **269**, 464 (2004)
- 7 J. Wu, S. Liu, *Adv. Mater.* **14**, 215 (2002)
- 8 Z. Wang, X. Qian, J. Yin, Z. Zhu, *Langmuir* **20**, 3441 (2004)
- 9 H. Yu, Z. Zhang, M. Han, X. Hao, F. Zhu, *J. Am. Chem. Soc.* **127**, 2378 (2005)
- 10 L. Vayssieres, *Adv. Mater.* **15**, 464 (2003)
- 11 R. Peterson, C. Fields, B. Gregg, *Langmuir* **20**, 5114 (2004)
- 12 Z. Tian, J. Voigt, J. Liu, B. Mckenzie, M. Mcdermott, M. Rodriguez, H. Konishi, H. Xu, *Nat. Mater.* **2**, 821 (2003)
- 13 Z. Zhang, H. Yu, X. Shao, M. Han, *Chem. Eur. J.* **11**, 3149 (2005)
- 14 L. Vayssieres, K. Keis, S. Lindquist, A. Hagfeldt, *J. Phys. Chem.* **105**, 3350 (2001)
- 15 R. Laudies, A. Ballman, *J. Phys. Chem.* **64**, 688 (1960)
- 16 W. Li, E. Shi, W. Zhong, Z. Yin, *J. Cryst. Growth* **203**, 186 (1999)
- 17 J. Wu, S. Liu, *J. Phys. Chem.* **106**, 9546 (2002)
- 18 M. Fuller, *J. Appl. Phys.* **15**, 164 (1944)
- 19 J. Zhang, L. Sun, J. Yin, H. Su, C. Liao, C. Yan, *Chem. Mater.* **14**, 4172 (2002)
- 20 M. Huang, Y. Wu, H. Feick, N. Tran, E. Weber, P. Yang, *Adv. Mater.* **13**, 113 (2001)
- 21 B. Jin, S. Im, S. Lee, *Thin Solid Films* **366**, 107 (2000)
- 22 P. Xu, Y. Sun, C. Shi, F. Xu, H. Pan, *Nucl. Instrum. Methods Phys. Res. B* **199**, 286 (2003)
- 23 X. Fan, J. Lian, L. Zhao, Y. Liu, *Appl. Surf. Sci.* **252**, 420 (2005)
- 24 S. Mahamuni, K. Borgohain, B. Bendre, *J. Appl. Phys.* **85**, 2861 (1999)
- 25 K. Vanheusden, C. Seager, W. Warren, D. Tallant, J. Voigt, *J. Appl. Phys.* **79**, 7983 (1996)